AD-A055 994 SYRACUSE UNIV N Y DEPT OF ELECTRICAL ENGINEERING F/G 20/14
RAY STRUCTURE OF DUCTED MULTIPATH FOR AN LOS LINK.(U)
MAY 78 R H LANG F30602-75-C-0121

UNCLASSIFIED RADC-TR-78-123 NL

1 OF 1
AD
A055 994

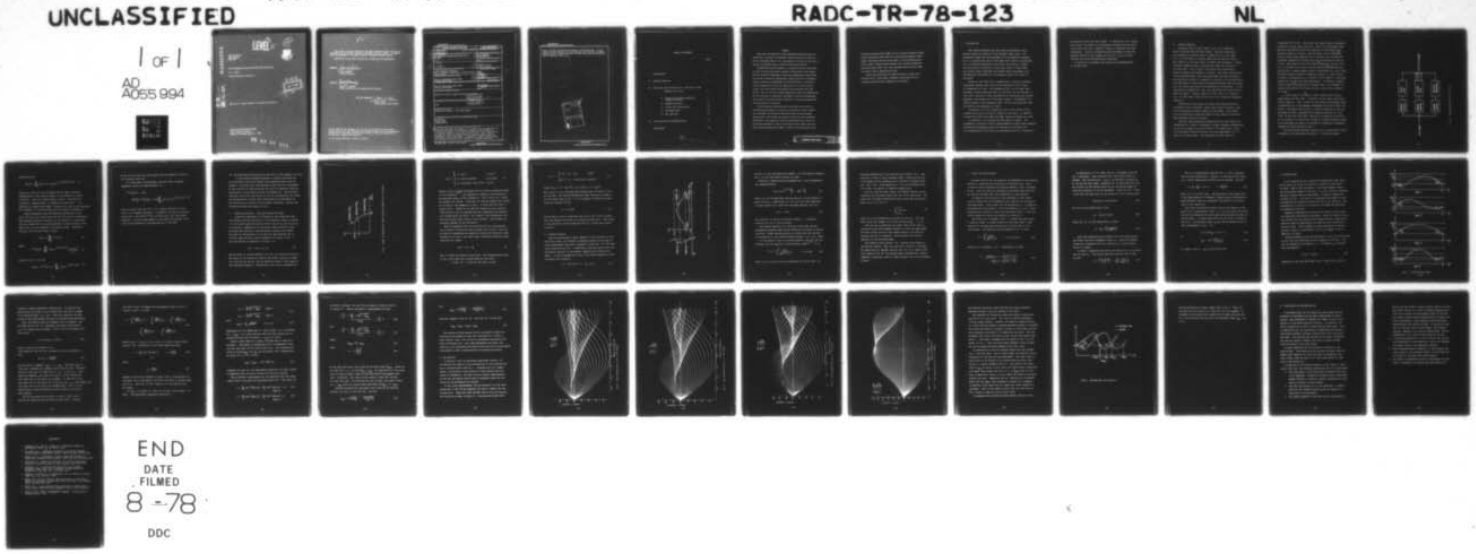

END
DATE
FILMED
8-78
DDC

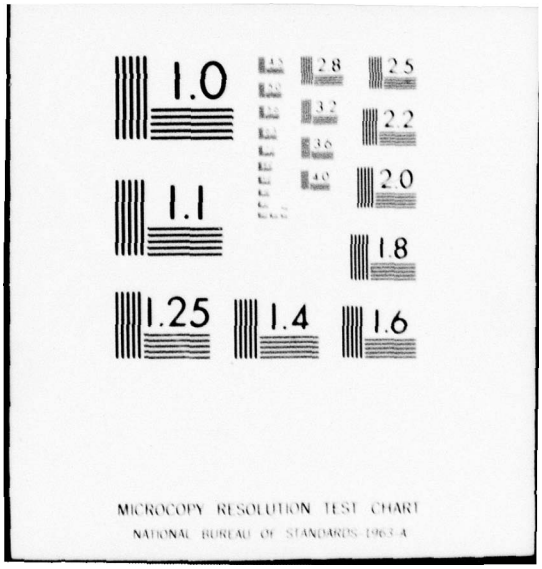
1.0
1.1
1.25
1.4
1.6
2.8
3.2
3.6
4.0
2.5
2.2
2.0
1.8
MICROCOPY RESOLUTION TEST CHART
NATIONAL BUREAU OF STANDARDS-1963-A

LEVEL II

RADC-TR-78-123
Phase Report
May 1978

RAY STRUCTURE OF DUCTED MULTIPATH FOR AN LOS LINK

R. H. Lang

George Washington University

Approved for public release; distribution unlimited.

ROME AIR DEVELOPMENT CENTER
Air Force Systems Command
Griffiss Air Force Base, New York 13441

This report has been reviewed by the RADC Information Office (OI) and is releasable to the National Technical Information Service (NTIS). At NTIS it will be releasable to the general public, including foreign nations.

RADC-TR-78-123 has been reviewed and is approved for publication.

APPROVED: Jacob Scherer

JACOB SCHERER
Project Engineer

APPROVED: Joseph J. Naresky

JOSEPH J. NARESKY
Chief, Reliability and Compatibility Division

FOR THE COMMANDER: John P. Huss

JOHN P. HUSS
Acting Chief, Plans Office

If your address has changed or if you wish to be removed from the RADC mailing list, or if the addressee is no longer employed by your organization, please notify RADC (RBC), Griffiss AFB NY 13441. This will assist us in maintaining a current mailing list.

Do not return this copy. Retain or destroy.

UNCLASSIFIED

SECURITY CLASSIFICATION OF THIS PAGE (When Data Entered)

REPORT DOCUMENTATION PAGE	READ INSTRUCTIONS BEFORE COMPLETING FORM
1. REPORT NUMBER: RADC-TR-78-123	2. GOVT ACCESSION NO. / 3. RECIPIENT'S CATALOG NUMBER
4. TITLE (and Subtitle): RAY STRUCTURE OF DUCTED MULTIPATH FOR AN LOS LINK.	5. TYPE OF REPORT & PERIOD COVERED: Phase Report.
	6. PERFORMING ORG. REPORT NUMBER: N/A
7. AUTHOR(s): R. H. Lang	8. CONTRACT OR GRANT NUMBER(s): F30602-75-C-0121
9. PERFORMING ORGANIZATION NAME AND ADDRESS: George Washington University, Dept of Electrical Engineering & Computer Science, Wash DC 20052	10. PROGRAM ELEMENT, PROJECT, TASK AREA & WORK UNIT NUMBERS: ~~920W~~ 95670016
11. CONTROLLING OFFICE NAME AND ADDRESS: Rome Air Development Center (RBC), Griffiss AFB NY 13441	12. REPORT DATE: May 1978 / 13. NUMBER OF PAGES: 34
14. MONITORING AGENCY NAME & ADDRESS (if different from Controlling Office): Rome Air Development Center (RBC), Griffiss AFB NY 13441	15. SECURITY CLASS. (of this report): UNCLASSIFIED / 15a. DECLASSIFICATION/DOWNGRADING SCHEDULE: N/A

16. DISTRIBUTION STATEMENT (of this Report)

Approved for public release; distribution unlimited.

17. DISTRIBUTION STATEMENT (of the abstract entered in Block 20, if different from Report)

Same

18. SUPPLEMENTARY NOTES

RADC Project Engineer: Jacob (NMI) Scherer

19. KEY WORDS (Continue on reverse side if necessary and identify by block number)

Propagation
Line-of-sight
Communications

20. ABSTRACT (Continue on reverse side if necessary and identify by block number)

This report describes the geometric optic analysis of a duct model for line-of-sight (LOS) fading. The atmospheric refractive index is modeled by three linear segments so as to form an elevated duct. The earth's curvature is taken into account by using the modified refractive index. Simple approximate formula are developed for the number of geometric-optic rays received for a given link length. In addition, the angle of departure from the transmitter of these rays is calculated. The angles enable one to

DD FORM 1 JAN 73 1473 EDITION OF 1 NOV 65 IS OBSOLETE

UNCLASSIFIED

SECURITY CLASSIFICATION OF THIS PAGE (When Data Entered)

339 712

readily calculate the amplitude and phase of contributing rays. To gain insight into the structure of the ray families, the trajectories of trapped rays are plotted. We have found that two cusps exist, each cusp having two caustics associated with it.

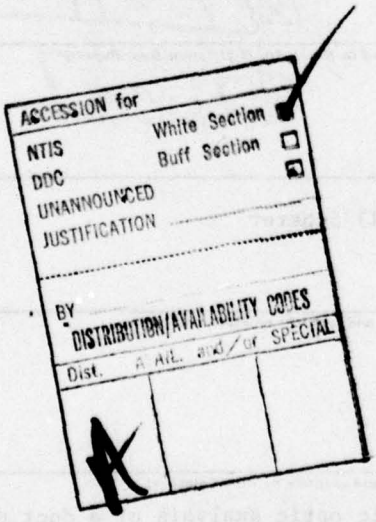

TABLE OF CONTENTS

PREFACE

This effort was conducted by George Washington University under the sponsorship of the Rome Air Development Center Post-Doctoral Program for Rome Air Development Center. Mr. Joseph Mensch of DCA was the task project engineer and provided overall technical direction and guidance.

The RADC Post-Doctoral Program is a cooperative venture between RADC and some sixty-five universities eligible to participate in the program. Syracuse University (Department of Electrical Engineering), Purdue University (School of Electrical Engineering), Georgia Institute of Technology (School of Electrical Engineering), and State University of New York at Buffalo (Department of Electrical Engineering) act as prime contractor schools with other schools participating via sub-contracts with prime schools. The U.S. Air Force Academy (Department of Electrical Engineering), Air Force Institute of Technology (Department of Electrical Engineering), and the Naval Post Graduate School (Department of Electrical Engineering) also participate in the program.

The Post-Doctoral Program provides an opportunity for faculty at participating universities to spend up to one year full time on exploratory development and problem-solving efforts with the post-doctorals splitting their time between the customer location and their educational institutions. The program is totally customer-funded with current projects being undertaken for Rome Air Development Center (RADC), Space and Missile Systems Organization (SAMSO), Aeronautical System Division (ASD),

Electronics Systems Division (ESD), Air Force Avionics Laboratory (AFAL), Foreign Technology Division (FTD), Air Force Weapons Laboratory (AFWL), Armament Development and Test Center (ADTC), Air Force Communications Service (AFCS), Aerospace Defense Command (ADC), HQ USAF, Defense Communications Agency (DCA), Navy, Army, Aerospace Medical Division (AMD), and Federal Aviation Administration (FAA).

Further information about the RADC Post-Doctoral Program can be obtained from Mr. Jacob Scherer, RADC/RBC, Griffiss AFB, NY 13441, telephone Autovon 587-2543, Commercial (315) 330-2543.

I Introduction

This report describes the work done on developing a propagation model for fading on line-of-sight (LOS) links. The propagation model has been developed with two specific purposes: first, to provide DCA with an LOS model that could be incorporated into its existing simulation facilities; and second, to determine the amount of selective fading that occurs in deep fades. The present report describes the general model development and the detailed calculations of the geometric-optic ray theory of multipath.

Fading on LOS links can be caused from a variety of physical mechanisms; however most links can be designed to avoid these or compensate for them. The atmosphere duct, on the other hand, provides a fading mechanism which is difficult for the designer to deal with. Because of their variability in occurrence and constant movement, they become one of the major causes of atmospheric induced outages on well designed links. We have thus based our fading model on the presence of a duct.

In section II of this report we give a brief review of the evidence that ducts can lead to fading on LOS links. In addition, we show that when these fades are deep, selective fading can occur.

In section III we develop the duct model in detail. The atmospheric refractive index is approximated by three linear segments. Following this, geometric-optics is employed to calculate the ray trajectories of the direct and multipath rays for a transmitter

and receiver having the same height. In particular, for a given link length, the number of contributing multipath rays is calculated along with their respective angles of departure from the transmitter. Finally a program has been developed to plot the complete family of rays trapped by the duct to aid in understanding the fading mechanism more completely.

In section IV we present the results and recommendations for further work.

II Channel Modeling

Microwave line of sight links in the 1 to 10 GHz band suffer from both slow and fast fading. The slow fading has a time constant of several hours or longer and is in the order of 1 to 10 db except in unusual cases such as blackout fading. Fast fading, on the other hand, is caused from multipath. Several different geometric-optic contributions reach the receiver at the same time. One of them is the direct wave contribution which the system was designed to recieve. The other contributions to the received signal come from waves that have been reflected from the earth surface or trapped in a surface or an elevated duct. The time delay of these other contributions differs from the direct wave and causes constructive and destructive interference. If the time delay is substantial, this can cause deep fast fading in the received signal. Usually fades are of the order of a second or two. In some cases, fades can be 30 to 40 db. deep and frequency selective.

Although the fast fading can occur from surface-reflection multipath or duct multipath, usually the surface reflection type can be eliminated by proper design of the system. This leaves duct contributions as the main cause of fast fading in the microwave frequency range of interest.

The fact that multipath was associated with fast fading was documented by a number of researches at Bell Telephone Laboratories in the late forties and early fifties.[1-3] In particular, Crawford and Jakes[1] performed angle of arrival experiments on a 22 mile link in New Jersey. They operated at about 4GHz with

a bandwidth of 450 MHZ. They found that under certain atmospheric conditions, severe fading occurred. During its occurrance, they observed that several waves were impinging on the antenna with different angles of arrival. Shortly after this De Lange[2] performed a short pulse experiment over the same link and observed multipath transmission effects with path differences as great as 7 feet. Much later in 1970 Bullington[4] related the vertical velocity of the duct to the fade rate and Ruthroff[5] demostrated that application of simple geometric-optic calculations to a duct could be used to predict Barnett's empirical result,i.e. that the distribution of attenuation is a function if L^3/λ where L is the path length and λ is the free space wavelength. In addition, several other authors[6,7] corrobarated the evidence that in the absense of surface reflections, ducts were the main cause of fast fading on LOS links.

In 1974, Bello et al[8] wrote a report dealing with digital modem design for LOS links. A portion of this report dealt with channel modeling. Here a model for LOS fading was presented which incorporated all of the physical mechanisms that could affect LOS fading. The model shown in Fig 1., which is similiar to the one presented by Bello, represents the transfer function for a LOS link. We see that the signal leaving the transmitter can arrive at the receiver via the direct, ducted or surface reflection paths. Along each path the signal is affected by atmospheric turbulence-labeled as volume scatter in Fig. 1.

The time varying transfer function T(f,t) relates the Fourier transform of the input and the output. It can be expressed

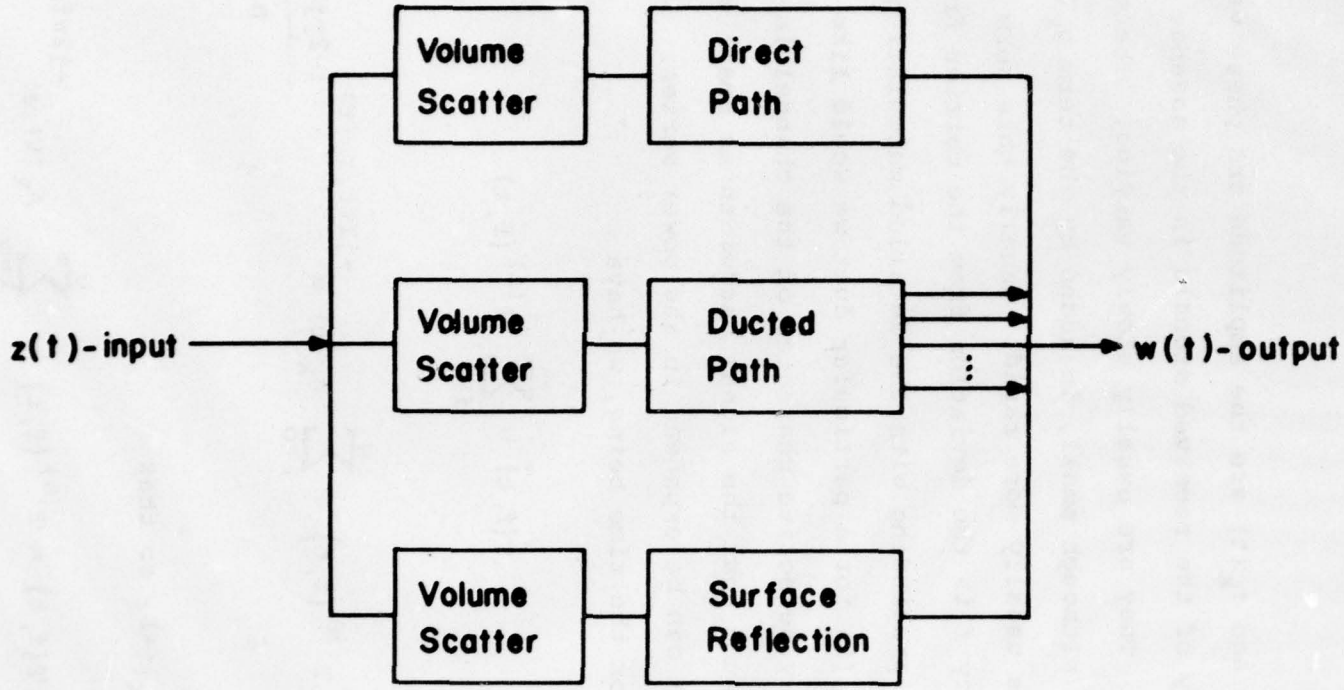

Fig 1. Multipath Model for LOS Link

analytically as

$$T(f,t) = \sum_{k=o}^{N} A_k(t) \left[1 + g_k(t)\right] e^{-j2\pi(f_0+f)\tau_k(t)} \qquad (1)$$

where $A_k(t)$ and $\tau_k(t)$ are the amplitude and phase variation respectively of the received signals in the absence of volume scattering. They are usually slowly varying. The effect of turbulence, although small, is added by the term $g_k(t)$. Its variation is usually more rapid. Usually this term can be neglected. The frequency f is the deviation from the carrier frequency f_0.

Before proceeding with the detailed calculations of the $A_k(t)$ and $\tau_k(t)$ for a particular duct we would like to demonstrate the frequency selective character of the channel in a deep fade. First we assume that the signal bandwidth is small enough so that $\exp(-j2\pi f\tau_k)$ can be expanded in the power series. Neglecting the $g_k(t)$ for the time being, we have

$$T(f,t) = \sum_{i=0}^{\infty} T^{(i)}(f,t) \qquad (2)$$

where

$$T^{(i)}(f,t) = \sum_{k=o}^{N} A_k(t)\, e^{-j2\pi f_0\tau_k(t)} \frac{(-2\pi j f\tau_k)^2}{n!} \qquad (3)$$

Usually $|f\tau_k| \ll 1$, so that

$$T(f,t) \simeq T^{(o)}(f,t) = \sum_{k=o}^{N} A_k(t)\, e^{-j2\pi f_0\tau_k(t)} \qquad (4)$$

We see in this case that the channel does not depend on f and is not frequency selective.

If a deep fade is encountered, the zero order multipath components cancel out approximately i.e.,

$T^{(o)}(f,t) \approx o$. Then

$$T(f,t) \approx T^{(1)}(f,t) = -2\pi jf \sum_{k=o}^{N} A_k(t)\tau_k(t)e^{-j2\pi f_o \tau_k(t)} \quad (5)$$

Here we clearly see that T(f,t) is a linear function of f and thus it is frequency selective. In addition, we notice the interesting fact, that since $T^{(o)}(f,t) \approx 0$, the $g_k(t)$ will now become important. We would thus expect to see rapid fluctuations in the order of milliseconds in the deep portion of the fade.

III Multipath Ray Structure for an LOS Link in the Presense of a Duct.

In this section geometric-optics is used to calculate the ray structure of the wave leaving the transmitter when a duct is present. Following this, the particular rays that are intercepted by the receiver are identified and the angle of departure from the transmitter is calculated for each intercepted ray. The difficult task here is not the calculation of the ray trajectories; but rather the determination of which rays trajectories are intercepted by the receiver as a function of duct height, thickness, receiver and transmitter height and length of link.

A. Problem Formulation - Modified Refractive Index

A realistic discussion of multipath on LOS links must take into account both the variation in the refractive index $n(z)$ where z is the height above the earth's surface as well as the curvature of the earth. Addressing the refractive index variation first, we assume the refractive index decreases linearly with height. The layer is incorporated in the model by approximating the refractive index by three linear segments as is shown in Fig. 2. Here the abcissa is measured in N units, i.e.

$$N(z) = (n(z) - 1)\ 10^6 \tag{6}$$

and the layer is located between h and $h+w$; the layer width being w. The value of the refractive index on the earth's surface is taken as N_0 and $\Delta N_1, \Delta N_2$ and ΔN_3 are the absolute values of the slopes of the individual segments. Analytically, $N(z)$ can be expressed as:

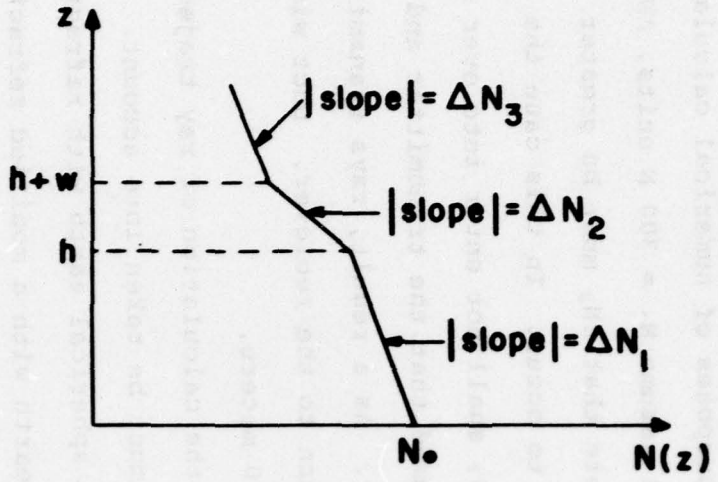

Fig 2. Model of Refractive Index Variation When Duct is Present.

$$N(z) = \begin{cases} N_0 - \Delta N_1 z & , \; 0 \leq z \leq h \\ N_0 - \Delta N_1 h - \Delta N_2 (z-h) & , \; h \leq z \leq h+w \\ N_0 - \Delta N_1 h - \Delta N_2 w - \Delta N_3 (z-h-w) & , \; z \geq h+w \end{cases} \qquad (7)$$

Typical values of these parameters can be found in numerous places in the literature[8]. For purposes of numerical calculations to be performed later, we shall assume $N_0 = 300$ N units, $\Delta N_1 = 40/km$ and $160/km < \Delta N_2 < 400/km$. Note that ΔN_2 must be greater than $157/km$ for ducting or ray trapping to occur. In this case the layer is called a duct. Values of ΔN_3 shall not enter into over calculations since it will be assumed that the transmitter and receiver are located below the layer. As a result, rays transmitted into the third region never return to the reciever. Duct widths are typically between 40 and 300 meters.

Before proceeding with the calculation of ray trajectories, the curvature of the earth must be taken into account. This can be done by transforming the spherical earth with refractive index variation n(z) into a flat earth with a modified refractive index variation m(z) where

$$m(z) = n(z) + \frac{z}{a} \qquad (8)$$

with "a" being the radius of the earth. The transformation given in (8) is not exact but is quite good for LOS links.

If eqs. (6), (7) and (8) are used, we find

$$m(z) = \begin{cases} m_1(z) = m_0 + g_0 z & , \ 0 \leq z \leq h \\ m_2(z) = m_0 + g_0 h - g_1 (z-h) & , \ h \leq z \leq h+w \end{cases} \tag{9}$$

where the $g_i = a^{-1} - \Delta N_i 10^{-6}$, i=1,2 and $m_0 = 1 + N_0 10^{-6}$

Note that m(z) for z>h+w has been omitted from (9) since it will not be used. The modified refractive index variation is shown on the left hand side of Fig. 3. It is plotted in terms of M units which are related to m by

$$M = (m-1)10^6 \tag{10}$$

We see that g_1 must be less than zero ($g_1 < 0$) for a duct to exist. Thus the minimum value that ΔN_2 can have is when $g_1 = 0$. This leads to the previously stated condition that $\Delta N_2 > 157$/km for ducting to occur.

B. Geometric-Optics

When the wavelength is small compared to the variation in the refractive index, the methods of geometric-optics can be used to obtain approximate solutions to Maxwell's equations. For LOS links these conditions are met. In addition, since the waves travel approximately parallel to the ground, depolarization effects are small. It can be assumed that each of the field components Ψ obey the scalar wave equation:

$$[\nabla^2 + k_0^2 m^2(z)] \Psi = 0 \ , \ k_0 = \omega/c_0 \tag{11}$$

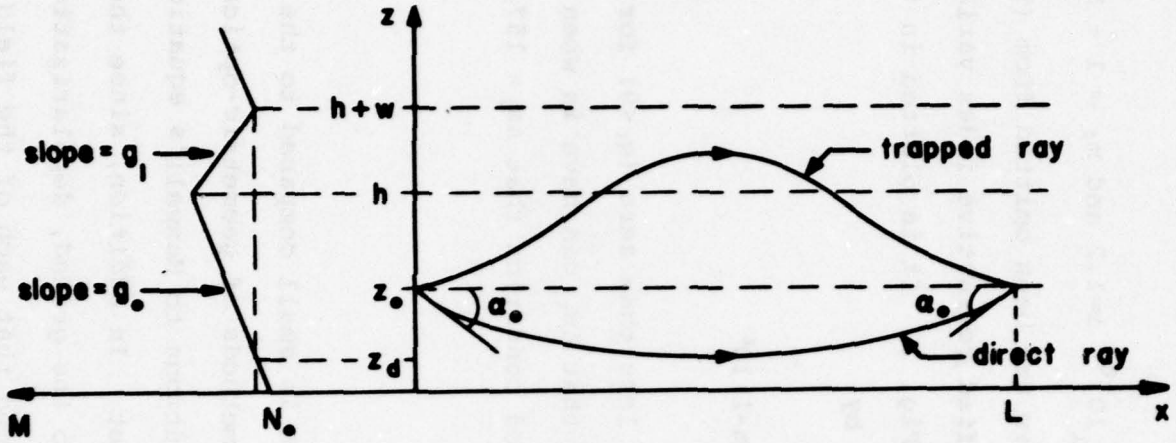

Fig 3. Modified Refractive Index and Two Typical Rays.

where k_0 is the free space wave number, ω is the angular frequency and c_0 is the free space velocity of light.

Basically, geometric-optics assumes that Ψ can be asymptotically approximated by

$$\Psi(\underline{r}) \sim A(\underline{r}) e^{ik_0\phi(\underline{r})}\left(1 + O\left(k_0^{-1}\right)\right) \tag{12}$$

where $A(\underline{r})$ is the amplitude function and $\phi(\underline{r})$ is the eikonal or phase function. Substitution of (12) into (11) and comparison of equal powers of k_0 gives the following equation for $\phi(r)$:

$$(\nabla\phi)^2 = m^2(z) \tag{13}$$

This equation is called the eikonal equation. A transport equation for $A(\underline{r})$ is also obtained.

The eikonal equation is a nonlinear first order partial differential equation that can be solved by the method of characteristics. These characteristics are called the rays and they are orthogonal to the constant phase surfaces, i.e., $\phi(\underline{r}) = \text{const.}$

For the special case of stratified medium, which we are considering, the ray equation is particularily simple.[9] It is

$$x = x_s \pm \int_{z_i}^{z} \frac{\sigma\, dz'}{\sqrt{m^2(z') - \sigma^2}} \qquad \sigma = m(z)\cos\alpha \tag{14}$$

where (x_i, z_i) are the initial coordinates of the ray and α is

the angle between the x axis and the ray at point (x,z). The function $m(z)\cos\alpha(z)$ has a constant value σ along any one ray. It is called the ray parameter and it serves to identify each ray. The + and - signs appearing in (14) are used when dx/dz (ray slope) is positive or negative respectively.

Once the rays have been found, the eikonal equation can be integrated and the phase along each ray can be calculated. The result for the phase accumulation along a ray from its initial point (x_i, z_i) to (x,z) is

$$\phi = \int_{(x_i,z_i)}^{(x,z)} m(z')ds \tag{15}$$

where ds is the differential arclength on the ray. The time delay along this segment of the ray is then simply $\tau = \phi/c_0$.

Once the ray trajectories are found, they can be used in conjunction with the transport equation to find the amplitudes. The basic result found is that energy inside a ray tube surrounding the ray is conserved. This principle can then be employed to find the amplitudes.

The geometric-optic ansatz, (12), remains valid except in diffraction regions. When the rays form a caustic or envelope, the amplitude $A(\underline{r})$ becomes infinite and (12) is no longer valid. Such regions occur for the problem under consideration, however asymptotic solutions, valid in these regions, will not be developed here.

C Direct Ray Calculations

We shall now use the ray equation (14) presented in the previous section to calculate the trajectory of the direct ray. This is the ray that intercepts the receiver whether a duct is present or not. Most LOS links are designed on the basis that this will be the only ray path from the transmitter to the receiver.

To simplify calculations for the remainder of this report we will assume that the transmitter and receiver are located at the same height. This height will be denoted by z_0. In addition, we assume that they remain in the first medium, i.e., $z_0 < h$. This configuration is shown in the right hand side of Fig. 3. The distance between the source and receiver is taken as L.

The direct ray, as shown in Fig. 3., leaves the source with a negative slope; it forms an angle α_0 with the x axis. This angle can't be determined now but will be found when L and α_0 are related. Now employing the ray equation (14), we have

$$x = -\int_{z_0}^{z} \frac{\sigma \, dz'}{\sqrt{m_1^2(z') - \sigma^2}} \quad , \sigma = m_1(z_0)\cos\alpha_0 \tag{16}$$

where $m_1(z)$ is defined in (9). Integrating, we find

$$x = \frac{\sigma}{g_0}\left\{\ln\left[m_1(z_0) + \sqrt{m_1^2(z_0) - \sigma^2}\right] - \ln\left[m_1(z) + \sqrt{m_1^2(z) - \sigma^2}\right]\right\} \tag{17}$$

An examination of (17) shows that as x increases along the ray, z decreases. This continues until the turning point is reached. The turning point, (x_t, z_t), is the point at which $\alpha=o$ or the ray has zero slope. Equation (17) is only valid for $x<x_t$. The location of the turning point can be calculated simply by using the constancy of the ray parameter σ along the ray. Since σ must have the same value at the source as at the turning point

$$m_1(z_t)\cos\alpha = m_1(z_0)\cos\alpha_0 \tag{18}$$

But $\alpha=o$ at the turning point, thus

$$z_t = \left(m_1(z_0) - m_0\right)/g_0 \tag{19}$$

Using (19) in (17) and simplifying, we have.

$$x_t = \frac{\sigma}{g_0} \ln\left(\frac{1 + \sin\alpha_0}{\cos\alpha_0}\right) \tag{20}$$

Since the transmitter and reciever are at the same height, the direct ray must be symmetric about x_t. Thus this symmetry allows us to determine the ray trajectory for $x_t \leq x \leq L$ without using (14) again.

In order to determine the direct ray explicitly, it is necessary to know α_0. This can be obtained from (20) since $L=2x_t$. We find

$$L = \frac{2m_1(z_0)\cos\alpha_0}{g_0} \ln\left(\frac{1 + \sin\alpha_0}{\cos\alpha_0}\right) \tag{21}$$

This is a transcendental equation for α_0, and in general, must be solved numerically: However, in the case of LOS links, $\alpha_0 << 1$, and an approximate solution can be obtained. We find:

$$\alpha_0 = \frac{L}{\Omega} + \frac{L^3}{3\Omega^3} + O(L/\Omega), \qquad \Omega = \frac{2m_1(z_0)}{g_0} \tag{22}$$

where $L/\Omega << 1$ for LOS links. The retention of the second term in the approximation is necessary, because phase differences between different rays are considered, the effects of the first term in (22) cancel out.

Once final consideration before leaving the subject of the direct ray is the blackout angle. If α_0 is too large, the direct ray will be reflected from the ground before passing through its turning point. To insure that this will not occur, we require that $z_t > o$. The blackout angle α_{OB} can now be defined as the α_0 that corresponds to $z_t = 0$, i.e.,

$$m_1(z_0)\cos\alpha_{OB} = m_1(0) = m_0 \tag{23}$$

or

$$\alpha_{OB} = \cos^{-1}\left(\frac{m_0}{m_1(z_0)}\right) \tag{24}$$

We require that $\alpha_0 < \alpha_{OB}$ for the direct ray.

D. Multipath Rays

In this section we will consider the additional paths along which energy can reach the receiver in addition to the direct ray path. When a duct is present, as we have assumed, some of the rays become trapped in the duct; for many receiver locations several of these rays are intercepted. A typical trapped ray is shown in Fig 3. Our goal is to determine the number of rays intercepting the receiver location and the α_0 for each ray. The knowledge of α_0 allows us to calculate the phase and amplitude contributed by each ray.

Geometric considerations indicate that there are four basic ray types that contribute to multipath. These are shown in Fig. 4. They account for rays leaving the transmitter with a positive or negative slope and approaching the receiver with a positive or negative slope. Other trapped ray types consisting of several periods of Type 1-4 are possible, but do not appear to be as important as these.

Before proceeding with the particulars of the ray calculations, we will find the conditions for ray trapping in the duct. The duct is defined as the region $z_d < z < h+w$ where z_d is defined from the equation

$$m_1(z_d) = m_2(h+w) \tag{25}$$

Reference to the left hand side of Fig 3 shows that z_d can be

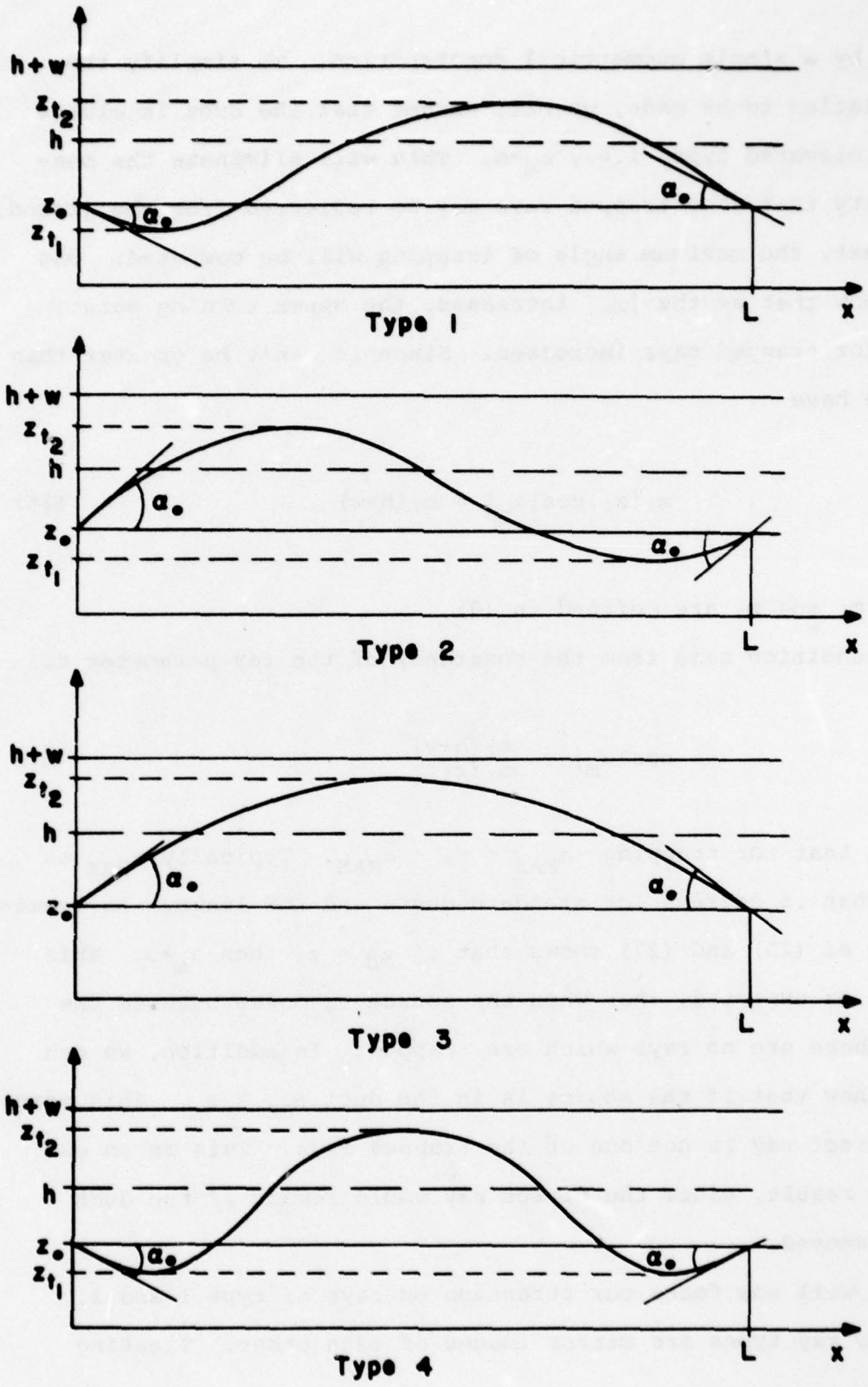

Fig 4. Multipath Ray Types

found by a simple geometrical construction. To simplify the calculation to be made, we will assume that the duct is always of an elevated type, i.e., $z_d > o$. This will eliminate the possibility that some trapped rays may be reflected from the ground.

Next, the maximum angle of trapping will be computed. One can show that as the $|\alpha_0|$ increases, the upper turning point, Z_{t_2}, for trapped rays increases. Since it can't be greater than h+w we have

$$m_1(z_0)\cos|\alpha_m| = m_2(h+w) \tag{26}$$

where m_1 and m_2 are defined in (9).
This condition came from the constancy of the ray parameter σ. Thus

$$\cos|\alpha_m| = \frac{m_2(h+w)}{m_1(z_0)} \tag{27}$$

We see that for trapping $-\alpha_{MAX} < \alpha_0 < \alpha_{MAX}$. Typically α_{MAX} is less than .5 degrees for standard ducts and LOS links. An examination of (25) and (27) shows that if $z_d = z_0$ then $\alpha_m = o$. This means, as expected, that when the source z_0 moves outside the duct there are no rays which are trapped. In addition, we can also show that if the source is in the duct $\alpha_{OB} > \alpha_m$. This means that the direct ray is not one of the trapped rays. This is an expected result, since the direct ray would remain if the duct were removed.

We will now focus our attention on rays of type 1 and 2. The two ray types are mirror images of each other. Treating

ray type 1 first, we employ the ray equation given in (14) to relate α_0 and L. We find

$$L = -\int_{z_0}^{z_{t_1}} \frac{\sigma dz'}{\sqrt{m_1^2(z')-\sigma^2}} + \int_{z_{t_1}}^{H} \frac{\sigma dz'}{\sqrt{m_1^2(z')-\sigma^2}} + \int_{h}^{z_{t_2}} \frac{\sigma dz'}{\sqrt{m_2^2(z')-\sigma^2}} \tag{28}$$

$$- \int_{z_{t_2}}^{h} \frac{dz'}{\sqrt{m_2^2(z')-\sigma^2}} - \int_{h}^{z_0} \frac{\sigma dz'}{\sqrt{m_2^2(z')-\sigma^2}}$$

where $m_1(z_{t_1}) = m_2(z_{t_2}) = m_1(z_0)\cos\alpha_0 = \sigma$ with m_1 and m_2 being given in (9). Integration of the above equations gives

$$L = \frac{2\sigma}{g_T}\cosh^{-1}\left(b\sec\alpha_0\right), \qquad b = \frac{m_1(h)}{m_1(z_0)} \tag{29}$$

$$\alpha_0 < o$$

where

$$g_T = \frac{g_0 g_1}{g_0+g_1} \tag{30}$$

Because of the mirror symmetry of type 1 and 2, the equation for the type 2 ray is the same as (28) with the terms in reverse order with $\alpha_0 > o$. Thus (29) is the L versus α_0 is the same for both ray types.

To find α_0 in terms of L from (29) we must again assume α_0 is small. The approximate expression obtained is

$$\alpha_{01} = -\frac{g_T}{2}\sqrt{L^2 - L_{MIN}^2} \qquad \text{(Type 1)}$$

$$\alpha_{02} = \frac{g_T}{2}\sqrt{L^2 - L_{MIN}^2} \qquad \text{(Type 2)} \tag{31}$$

with

$$L_{MIN} = \frac{2}{g_T}\sqrt{2g_0\Delta h} \qquad \Delta h = z_0 - h \tag{32}$$

Examination of (31) shows that no rays of type 1 or 2 contribute if $L < L_{MIN}$. In a later section, when the ray trajectories are plotted will see that the point $L = L_{MIN}$ is a focus.

Since a lower bound to L exists, we might ask if there is a maximum L. The answer is affirmative and it corresponds to the ray that has taken on the initial angle $|\alpha_m|$. This maximum distance is called L_{BM1} and L_{BM2} for ray types 1 and 2 respectively. By using (27) in (29), we find

$$L_{BM1} = L_{BM2} = 2\sqrt{2}\sqrt{g_1 w}/g_T \tag{33}$$

Although (31) and (33) are approximate expression for small angles of departure they are quite accurate for LOS calculations.

The α_0 versus L relationship for the remaining two rays types (type 3 and 4) can again be calculated using (14). The result is:

$$L = \frac{2\sigma}{g_T}\cosh^{-1}\left(b\sec\alpha_0\right) - \frac{2\sigma}{g_0}\cosh^{-1}\left(\sec\alpha_0\right), \quad \alpha_0 > 0 \tag{34}$$

(Type 3)

$$L = \frac{2\sigma}{g_T}\cosh^{-1}\left(b\sec\alpha_0\right) + \frac{2\sigma}{g_0}\cosh^{-1}\left(\sec\alpha_0\right), \quad \alpha_0 < 0 \tag{35}$$

(Type 4)

As before, although (34) and (35) are exact, we wish to find α_0 in terms of L. Making the small α_0 approximation we find

$$\alpha_{03}^{(\pm)} = \frac{\frac{g_T L}{g_0} \pm \sqrt{L^2 - \hat{L}_{MIN}^2}}{2t/g_T}, \quad \alpha_{03}^{(\pm)} > 0 \tag{36}$$

and

$$\alpha_{04}^{(\pm)} = -\frac{\frac{g_T L}{g_0} \pm \sqrt{L^2 - \hat{L}_{MIN}^2}}{2t/g_T}, \quad \alpha_{04}^{(\pm)} < 0 \tag{37}$$

where

$$\hat{L}_{MIN} = \sqrt{t}\ L_{MIN} \tag{38}$$

with

$$t = 1 - \left(\frac{g_T}{g_0}\right)^2 \tag{39}$$

We see that both type 3 and 4 rays do not exist when $L < \hat{L}_{MIN}$. Since one can show that $t \leq 1$, we have $\hat{L}_{MIN} \leq L_{MIN}$. An examination of (36) shows that two rays of type 3 exist if both $\alpha_{03}^{(+)}$ and $\alpha_{03}^{(-)}$ are greater than zero. Similarily, two rays of type 4 exist if both $\alpha_{04}^{(+)}$ and $\alpha_{04}^{(-)}$ are less than zero. We find that one ray of type 3 and type 4 exists if $L > L_{MIN}$ while two rays of each type exist if $\hat{L}_{MIN} < L < L_{MIN}$.

Maximum distances for rays type 3 and 4 also can be found by putting $|\alpha_0| = |\alpha_m|$ in (34) and (35). We find

$$L_{BM3} = 2\sqrt{2}\left(\sqrt{\frac{g_1 w}{g_T}} - \frac{\sqrt{g_1 w - g_0 \Delta h}}{g_0}\right) \tag{40}$$

and

$$L_{BM4} = 2\sqrt{2}\left(\frac{\sqrt{g_1 w}}{g_T} + \frac{\sqrt{g_1 w - g_0 \Delta h}}{g_0}\right) \tag{41}$$

From the algebraic form of (33), (40) and (41), we see that

$$L_{BM3} \leq L_{BM1} = L_{BM2} \leq L_{BM4} \tag{42}$$

The results of this section give us an explicit method for calculating the number of rays that contribute at a given L. These formula also give us the ray parameters associated with each contributing ray. Once these parameters are known, calculation of the time delay and phase along each path follows easily from geometric optic considerations as indicated previously.

E Ray Families

In section C and D we developed approximate formula for calculating the number of rays contributing to the received signal at any particular value of L. Although this is a needed result, our picture of the totality of rays emitted from the source is incomplete. We need to have a global understanding of how the rays behave and we need to determine where the coustics and ray boundaries are located.

To gain this understanding, the ray equation (14) was integrated and an IBM 370-148 computer was used to compute the ray trajectories. These were then plotted using a Zeta 230 plotter. The results are shown in Figs 4-7. The plots were made using

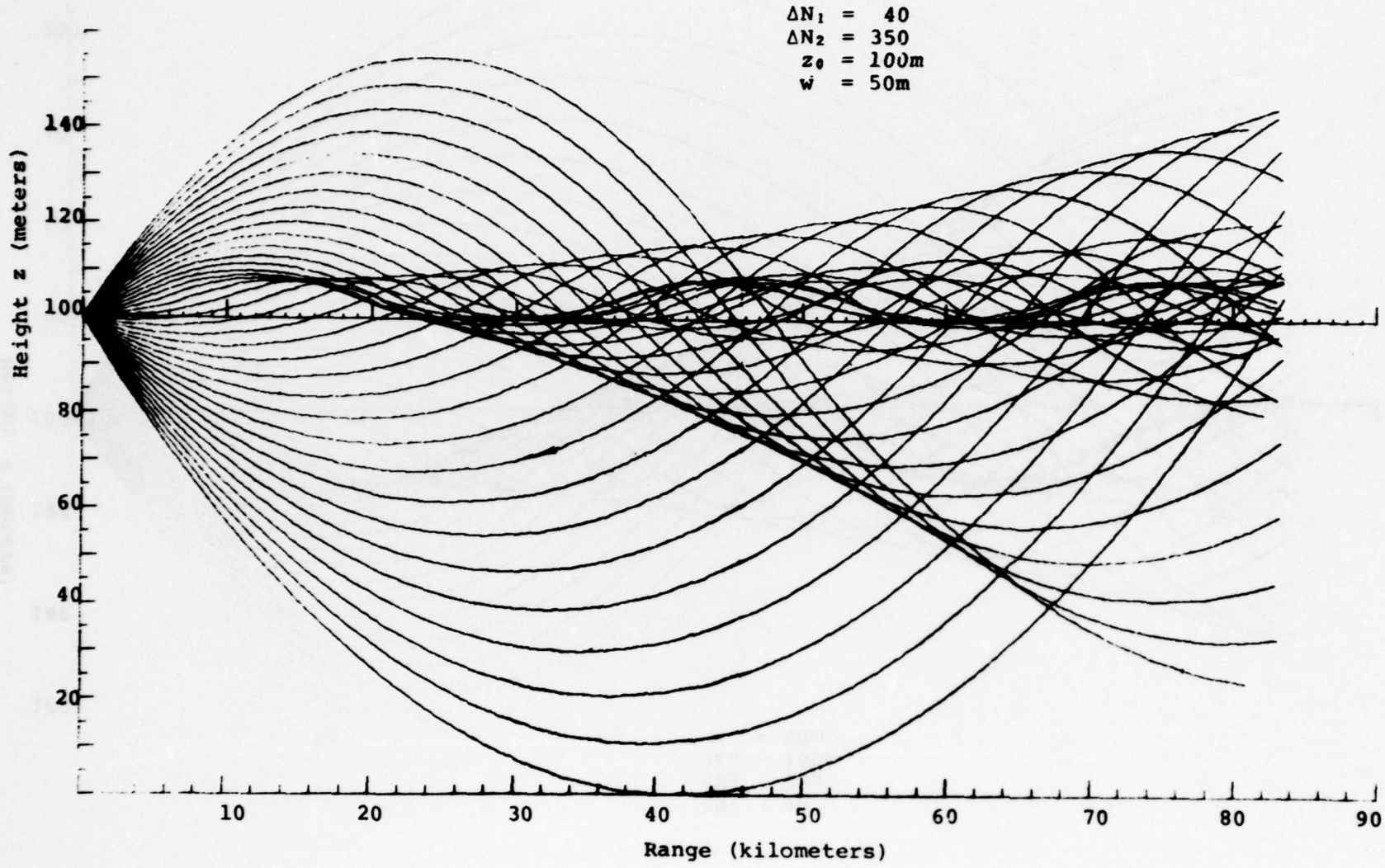

Fig 4. Ray Trajectories for h = 105 meters

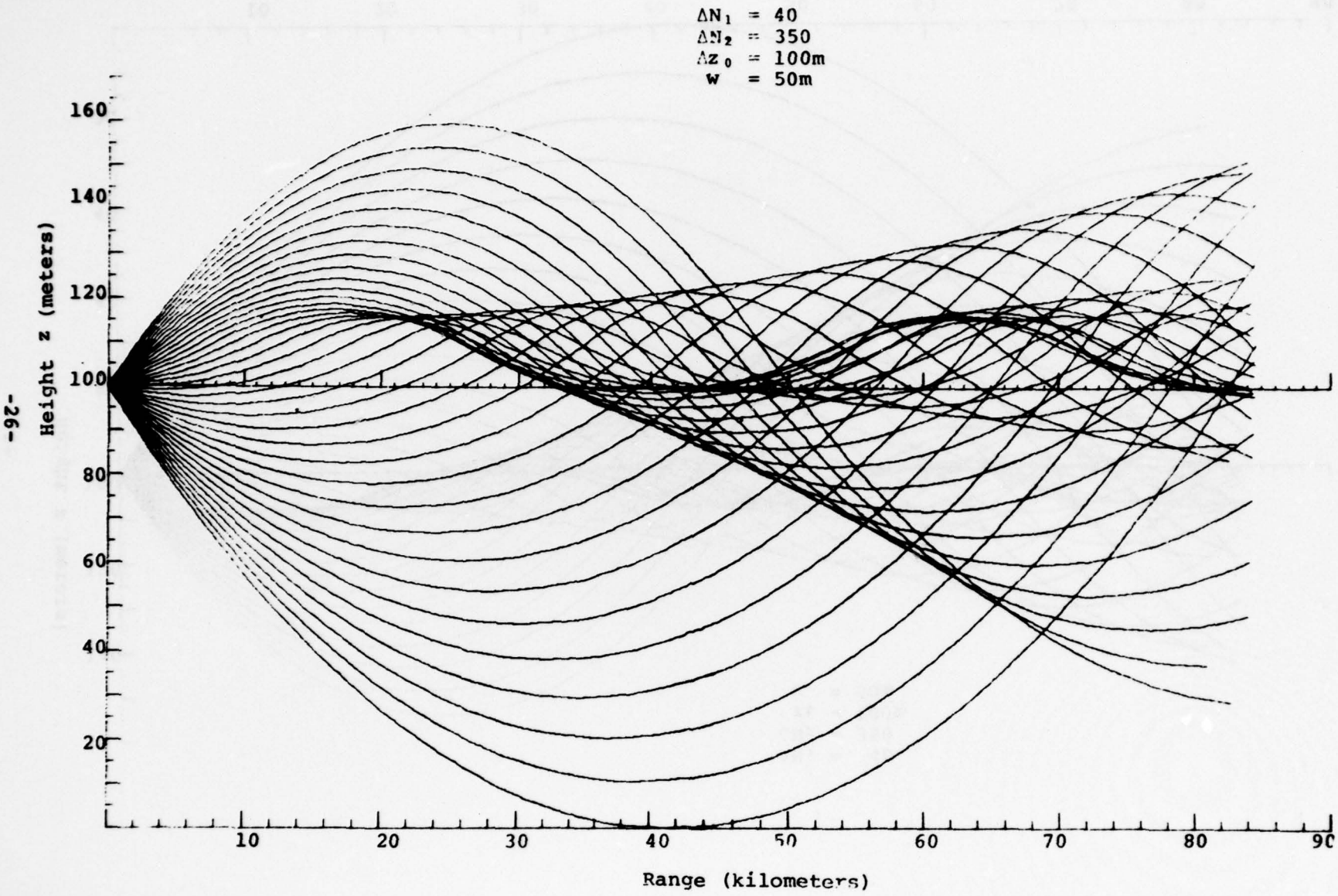

Fig 5 Ray Trajectories for h = 110 meters

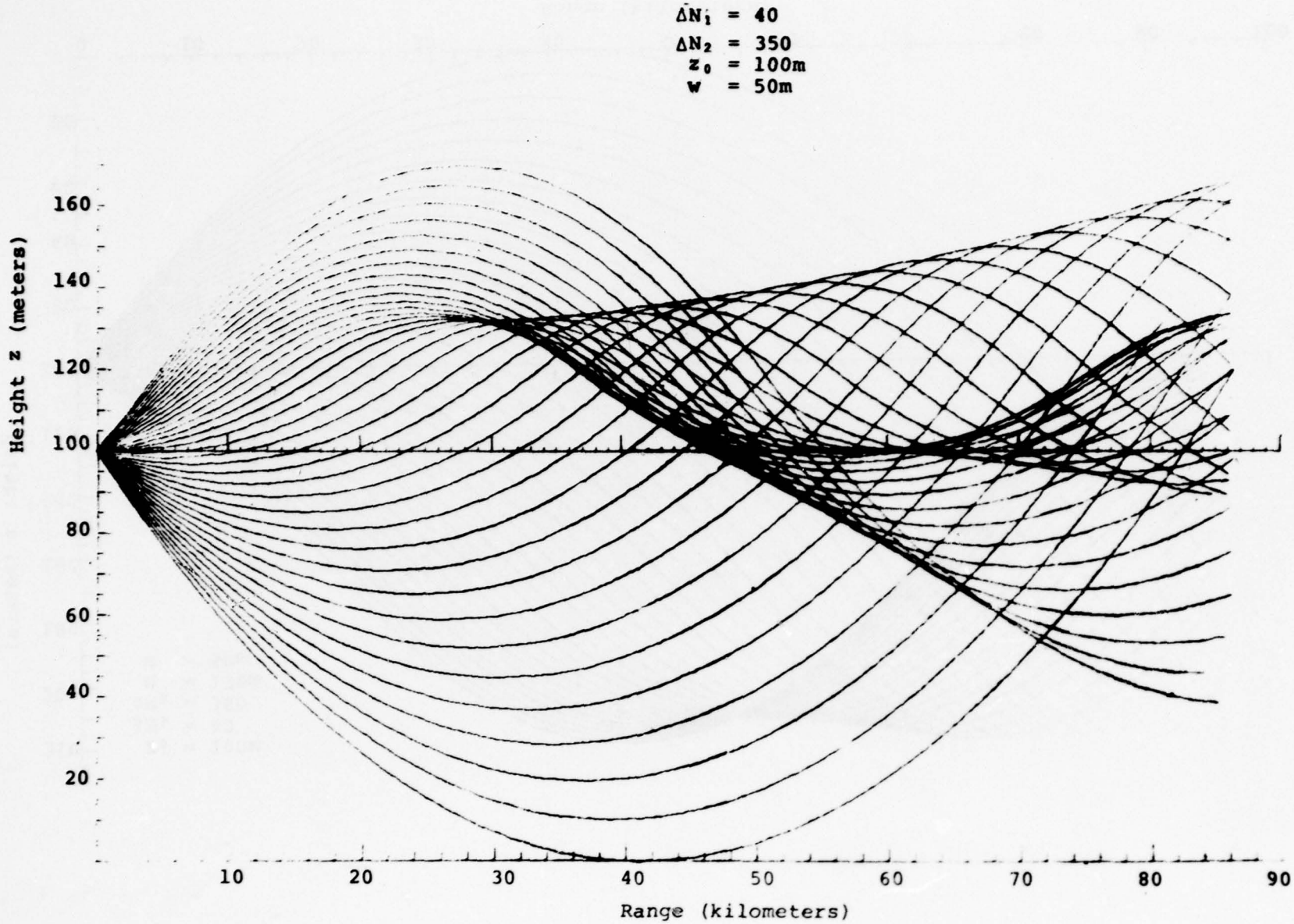

Fig 6. Ray Trajectories hor h = 120 meters

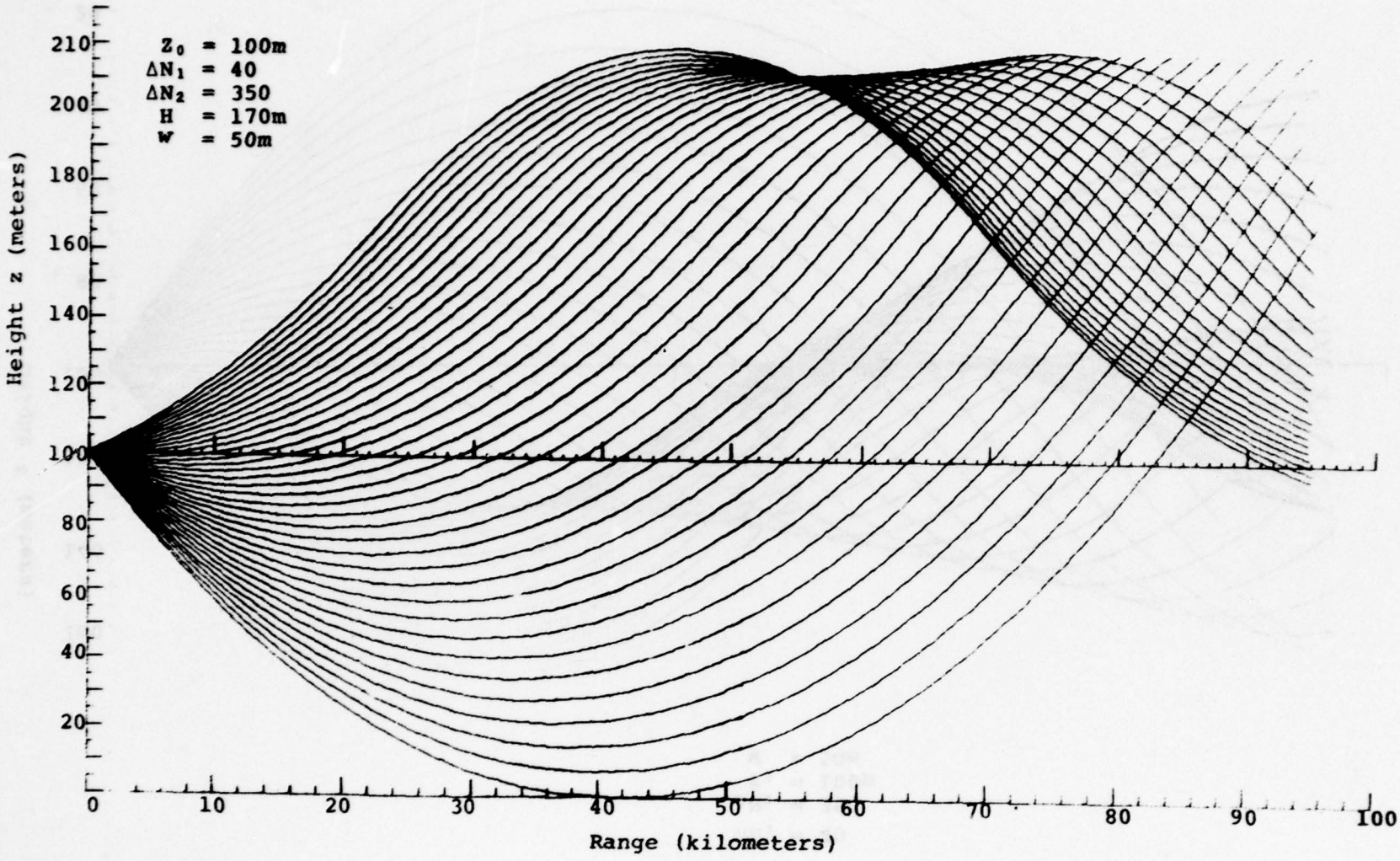

Fig 7. Ray Trajectories for h = 170 meters

the modified refractive index and thus the range coordinate measures distance along the surface of the earth.

The gradients of refractive index were taken as ΔN_1=40 and ΔN_2=350 for all four plots. The value of ΔN_2=350 represents a fairly steep gradient. However, we wished to examine ducting in a worst case environment (maximum measured gradient is ΔN_2=420). The source was held at a constant location of 100 meters and the duct parameter w was kept at 50 meters for all plots. The only parameter that varies from plot to plot is the duct height parameter h. The height increases from 105 meter in Fig. 4 to 170 meters in Fig 7. Thus the plots taken together, serve to show how the multipath structure changes as the duct rises.

An examination of the ray families shows that each (except Fig 7) has two cusps. Each of these cusps are formed by the intersection of two caustics (ray envelopes). The lower cusp always occurs at the height of the source while the other cusp occurs at a height somewhat above it. The range of the lower cusp in L_{MIN} as given in (32), while the lower caustic associated with upper cusp crosses the line $z = z_0$ at $\hat{L}_{MIN}$ given in (38). This is shown more clearly in Fig 8 where the caustics are shown without the rays. Inspecting the ray families as h increases shows that the upper cusp increases in height as h increases. In addition, both cusps occur at larger and larger ranges as h increases. This is the reason we don't see the lower cusp in Fig 7 since it occurs at such a large range.

To complete the interrelationship between section D and E;

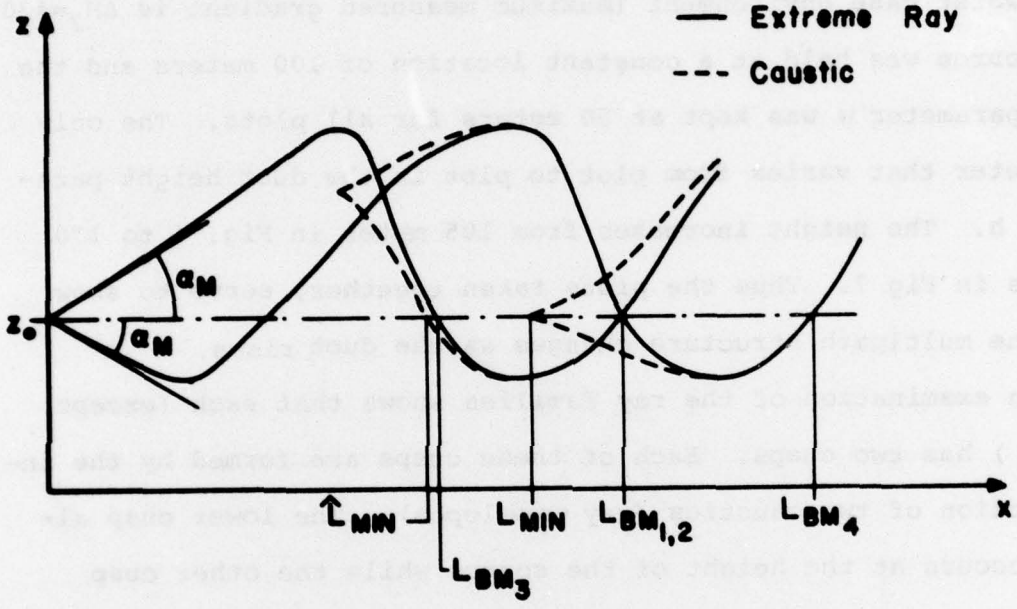

Fig 8. Extreme Rays and Caustics.

we have plotted the extreme trapped rays in Fig 8. These are the rays with the largest $|\alpha_0|$ that will still be trapped. As is shown in this figure the intersection of these rays with the $z=z_0$ line coincides with the outer ray boundary ranges L_{BMi}, i=1, 2,3,4.

IV Conclusions and Recommendations

A tractable model for LOS fading has been chosen and the structure of multipath rays has been investigated in detail. Formula were determined to compute the number of rays contributing at a particular receiver location. In addition, the angle of departure of each of these rays has been found. This is important since the calculation of amplitudes and phases or time delays becomes a straight forward matter once the angles are known. The analysis was carried out for equal transmitter and receiver heights, however, the case of unequal heights could be treated in the same manner.

To help understand the ray structure, families of rays were plotted. From these plots we see that multipath rays are almost never observed on links less than 20 kilometers long while longer links can have 2 to 4 rays contributing in addition to the direct ray.

To make use of the results obtained in this report to simulate an LOS link, the following tasks would have to be performed:

1. the calculation of the amplitudes and phases would have to be completed. Because the geometric-optic amplitudes become infinite at caustics, special consideration would have to be given to these regions.
2. Once the calculations in (1) are completed, a computer code for the transfer function given in equation (1) would have to be developed.
3. The dynamic aspects of the model can be introduced by

making the duct height a slowly varying function of time. This might consist of a slowly increasing deterministic function to account for the gradual rising of the duct and a small slowly varying random portion to account for local fluctuations. Some comparison with statistical meteorological data should be made. It should be noted that for each new value of duct height, the transfer function computed in (2) must be recalculated. The implementation of (2) must be fast enough to do this.

4. If diversity operation is to be simulated, the calculations performed in this report will have to be extended to unequal receiver and transmitter heights.
5. Since implementation of equation (1) would require the input signal in the frequency domain, an FFT would have to be done on the input and output signals.
6. The effect of turbulence could be incorporated into the model to determine its effects when deep fades occur.

REFERENCES

1. Crawford, A.B. and W.C. Jakes, Jr., "Selective Fading of Microwaves", BSTJ, 31, pp. 68-90, 1952.

2. De Lange, O.E., "Propagation Studies at Microwave Frequencies by Means of Very Short Pulses", BSTS, 31, pp. 91-103,1952.

3 Kaylor, R.L., "A Statistical Study of Selective Fading of Super-High Frequency Radio Signals", BSTJ, 32, pp. 1187-1202,1953.

4. Bullinton, K., "Phase and Amplitude Variation in Multipath Fading of Microwave Signals", BSTJ, 50, pp. 2039-2053, 1971.

5. Ruthroff, C.L., "Multiple-Path Fading on Line-of-Sight Microwave Radio Systems as a Function of Path Length and Frequency", BSTJ, 50. pp. 2375-2398, 1971.

6. Ikegami, "Influence of an Atmospheric Duct on Microwave Fading", IEEE, AP-S, pp. 252-257, 1959.

7. Moler, W.F. and W.A. Arvola, "Vertical Motion in the Atmosphere and its Effect on VHF Radio Signal Strength," Am. Geophys. Union, 37 p399-409, 1956.

8. Bello, P.A., et al, "Line-of-Sight Techniques Investigation", Final Report, RADC-TR-74-330, Chapter 1 and 2, 1975. (A006104)

9. Born, M and E. Wolfe, Principles of Optics. Fourth Edition, Pergamon Press, 1970.